As Symmetric As Possible : Shape Completion with Non-Rigid Registration Leveraging Generalized Cylinder Decomposition

Shuji Oishi[1], Masashi Yokozuka[1], Atsuhiko Banno[1]

***Abstract*— To infer a 3D entire shape from its partial observation, a non-rigid registration algorithm that employs embedded deformations is proposed. We construct a deformation graph on a reference model to discretize the space, and compute a complex deformation as a collection of affine transformations to align the reference model toward the given geometric data. To avoid distortion artifacts during the non-rigid registration, we introduce constraint "As symmetric as possible (ASAP)" on the graph via a generalized cylinder decomposition. ASAP allows model deformation maintaining its underlying local symmetry, which leads to plausible shape completion in the area with no observation. We performed experiments with synthesized data, and demonstrated that the proposed method successfully restored missing surfaces compared with conventional completion techniques.**

I. INTRODUCTION

Inferring complete 3D shapes of objects from a single view is important for autonomous robots to grab a structure of the scene. As robots capture geometric data with range sensors such as RGB-D cameras and laser scanners from a certain viewpoint, the region behind objects may be occluded. This incomplete observation creates uncertainty in understanding the surroundings, and results in, for example, inefficient path planning and awkward object manipulations. Therefore, the ability to infer the entire shape from partial cues allows robots to better understand the surroundings, leading to more stable task execution.

We humans can easily predict the entire 3D shape based on its partial observation. To imitate this sophisticated human visual perception, a variety of techniques have been developed to infer the underlying geometry, as shall be explained later in Section II. These shape completion techniques enable autonomous robots to perform complicated tasks based even on limited observations, for example, in robotic grasp planning employing occluded-shape inference[1][2] or in shape-uncertainty-driven tactile exploration[3]. In particular, the recent development of a non-rigid registration[4][5][6][7] makes it possible to generate a detailed complete 3D model by deforming a reference mesh model onto the given partial shape. However, a difficulty remains in recovering unseen surfaces from the partial cues because some parts of the reference model have no target to align with and a meaningful deformation is impossible.

*This work was supported by JSPS KAKENHI Grant Numbers 16K16084 and 18K18072, and a project commissioned by the New Energy and Industrial Technology Development Organization (NEDO).

[1]Smart Mobility Research Team, National Institute of Advanced Industrial Science and Technology (AIST), Tsukuba, Japan {shuji.oishi, yokotsuka-masashi, atsuhiko.banno}@aist.go.jp

In this paper, we propose a method that overcomes the drawback of non-rigid registration by leveraging symmetry extracted via the generalized cylinder decomposition[8]. Our method decomposes a reference model into a set of skeletal and cross-section profiles, and builds a symmetry-aware deformation graph by analyzing local symmetry based on the decomposition result. The deformation graph enables an "As Symmetric As Possible (ASAP)" constraint to be introduced in non-rigid registration, which leads to symmetry-aware model deformations to infer the missing surface better.

The main contribution of this paper is combining the model deformation and the symmetry assumption by leveraging the generalized cylinder decomposition for 3D shape completion, and hence allow for a more general non-rigid registration. Note that we are interested in a complete and detailed generation of a mesh model starting from a reference model the shape of which is moderately similar but not the same as the query, i.e., an object in the same category. Although conventional non-rigid registration techniques successfully reconstruct the full 3D model from a partial geometric form, they typically require highly similar reference models, which implicitly assumes the target and reference models (almost) describe the same objects. As another approach, data-driven techniques[9][10][11][2] have shown the ability to recover complete shapes only from partial cues; however, a large amount of relevant data is required for learning and the reconstruction results tend to have some undesirable artifacts. In contrast, the proposed method seeks to deform the reference model to align the partial observation while retaining the intrinsic geometry by introducing the ASAP constraint, which leads to high-quality completion from one example.

The rest of this paper is organized as follows. First, the previous shape completion approaches are reviewed in Section II to see the overview. In Section III, we describe the algorithm of our shape completion method including non-rigid registration, deformation graph construction via the generalized cylinder decomposition, and symmetry-aware model deformations. In Section IV, we show experimental results using synthesized data to quantitatively evaluate the performance of the proposed method, and also compared our method with other recent techniques.

II. RELATED WORK

Implicit surface: Implicit surface is one of several popular completion methods. By representing the object shape as a signed distance function (SDF) and extracting its zero isosurface by meshing techniques like the marching cubes, a

smooth and closed 3D model can be reconstructed. A variety of techniques such as those based on the compactly supported radial basis functions[12] is proposed to interpolate scattered point clouds. Concerning robotic applications, Gaussian process implicit surface (GPIS)[13], Bayesian representation of SDFs, has been employed to incorporate uncertainty in noisy observations[14][3]. However, implicit surface is only capable of dealing with small defects and not suitable for completing areas with no observation.

Symmetric duplication: To construct unseen surfaces, it may be effective to make some assumption as to the underlying geometry. Symmetry is one useful option to model organic objects and artifacts, in which partial observations are duplicated in another side. Bohg *et al*.[1] proposed a method to predict full shapes of manmade objects with symmetric duplication for reliable object grasping. It finds the optimal symmetry plane perpendicular to the tabletop on which the target objects are located by evaluating whether the mirrored points are consistent with the original points. A similar approach can be found in [15] followed by hole filling to complete the 3D models.

Speciale *et al*.[16] also developed a surface denoising and completion method making use of symmetries in a variational optimization framework for plausible 3D reconstruction. They first detect multiple planar symmetries that underlie an incomplete 3D model using random sample consensus (RANSAC) or Hough transform, and introduce them as a prior in the variation regularizer to reconstruct smooth and symmetric surfaces in a truncated signed distance function. While it leads to simultaneous denoising and completion, extracting accurate symmetry axes from limited observations is not always trivial. Moreover, the assumption works well on objects whose shapes can be described only by symmetric duplications of the partial observations.

Model fitting: When prior knowledge such as complete 3D model database is available, an entire shape of the target is easily recovered by aligning the same or similar 3D model in the database to the query depth data. This is the so-called "model fitting", which enables hidden surfaces to be inferred in detail. For example, Moreno *et al*.[17] developed a robust RGB-D SLAM that employed real-time object recognition and pre-constructed 3D model fitting using the iterative closest points (ICP) algorithm. Choi *et al*.[18] proposed a 6-DoF object tracking algorithm using an RGB-D camera parallelizing likelihood evaluations in particle filtering with a GPU for real-time accurate pose estimation. For semantic mapping, Zeng *et al*.[19] developed a simultaneous object detection and localization method employing conditional random field (CRF) methods to model contextual relations between objects and achieving significantly higher accuracy in object pose estimation. Model fitting, however, is applicable only to known objects for which prior 3D mesh models are given, and thus it is necessary to prepare the 3D models of all possible objects in advance.

Deformation: Relaxing the limitations of model fitting, deforming the reference model so that the surface well aligns with the given observation, is one promising approach. With simultaneous registration and deformation, it has the capability of generating highly detailed completed 3D models. Amberg *et al*.[20] proposed a deformation method that estimates an affine transformation on each vertex introducing a stiffness term to control the flexibility of the reference model. Similarly, Li *et al*.[4][5] presented non-rigid registration algorithms using embedded deformation[21] which efficiently and robustly solved complex deformations in a non-linear optimization. More recently, GPU-aided deformation[6] for realtime shape completion, and L1-norm regularized deformation[7] for robustness in large changes in posture have been proposed.

However, the methods require highly similar reference models, which implicitly assumes both target and reference mesh models represent (almost) the same objects. This implicit assumption allows us to neglect deformations of surfaces with no observations; vertices in the reference model having no correspondences are merely displaced to maintain smoothness and tend to remain in their original shape of the reference model. If the partial observation and reference model describes almost the same object, the reconstruction result might be fine.

In contrast, our work considers shape completion with more general non-rigid registration where shapes of the query and reference model are not the same, i.e., objects in the same category, and conventional non-rigid registration techniques might not be suitable for inferring the missing surfaces. The most similar technique to our method would be as-conformal-as-possible surface registration proposed by Yoshiyasu *et al*.[22]. They introduced an angle-preserving stiffness term in non-rigid registration to allow changes in local scale (similarity transformation) and enabled non-rigid registration between different size models. However, as is the case with other techniques, valid constraints are limited around partial observations.

III. As Symmetric As Possible Deformation

A. Overview

Whereas the model deformations allow us to reconstruct detailed complete 3D models by aligning and transforming a reference model, the hidden surfaces to be estimated tend to have almost the same shape as the original reference model. To make plausible deformations there, we also need to pose valid assumptions as mentioned in Section II to duplicate the displacements by analyzing the geometry.

This motivated us to develop a new completion approach the "as symmetric as possible (ASAP)" deformation. By extracting intrinsic symmetry in the reference model and building a symmetry-aware deformation graph, we enjoy the benefit of symmetric assumption in non-rigid registration (see Fig.1). In this section, we first describe a non-rigid registration algorithm based on embedded deformation[21], and then introduce the symmetric constraint derived from the generalized cylinder decomposition.

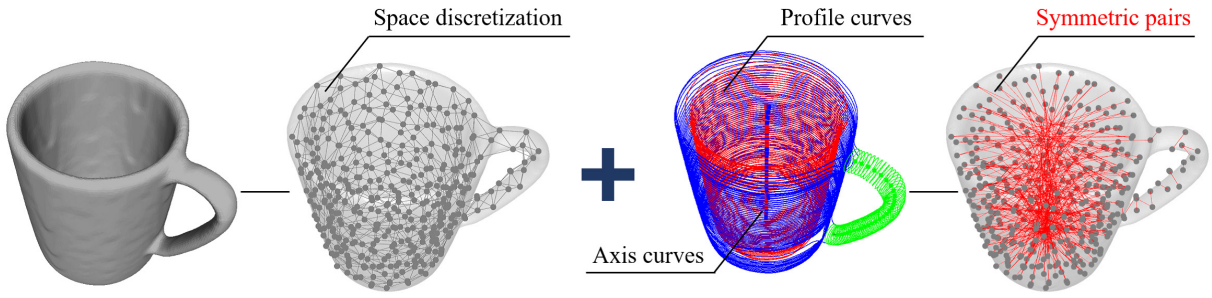

(a) Reference model (b) Embedded deformation graph (c) Generalized cylinder decomposition (d) Symmetry-aware graph

Fig. 1. Overview of As Symmetric As Possible (ASAP) deformation graph

B. Surface Deformation with Embedded Deformation

Inspired by [5], [4], and [22], we developed a non-rigid registration employing the embedded deformation[21] for robust and efficient surface registration. Embedded deformation discretizes the space by defining a deformation graph on the reference model (Fig.1(a),(b)) that computes complex deformations as a collection of transformations. Each node $\mathbf{x}_i \in \mathbb{R}^3, i \in 1 \cdots m$ of the embedded graph induces a local affine deformation specified by a 3×3 transformation matrix $\mathbf{A}_i$ and a 3×1 translation vector $\mathbf{t}_i$. Each vertex $\mathbf{v}_j \in \mathbb{R}^3, j \in 1 \cdots n$ of the reference model is mapped to the new position $\mathbf{v'}_j$ with influences from the surrounding nodes described as follows:

$$\mathbf{v'}_j = \sum_{\mathbf{x}_i} w(\mathbf{v}_j, \mathbf{x}_i) \left[\mathbf{A}_i (\mathbf{v}_j - \mathbf{x}_i) + \mathbf{x}_i + \mathbf{t}_i\right], \quad (1)$$

$$w(\mathbf{v}_j, \mathbf{x}_i) = |1 - d^2(\mathbf{v}_j, \mathbf{x}_i)/d^2_{max}|^3, \quad (2)$$

where $d(\mathbf{v}_j, \mathbf{x}_i)$ denotes the distance between $\mathbf{v}_j$ and $\mathbf{x}_i$, and d_{max} the distance from $\mathbf{v}_i$ to the farthest neighboring node. Following [5], we used geodesic distances instead of Euclidean distances to calculate $d(\mathbf{v}_j, \mathbf{x}_i)$ to avoid distortion artifacts during non-rigid registration.

The node-wise affine transformations $\mathbf{X}_i = [\mathbf{A}_i, \mathbf{t}_i], i \in 1 \cdots m$ are treated as unknowns to be solved in the non-rigid registration. The local features in the reference model should be preserved to avoid unnatural deformations, and therefore all $\mathbf{A}_i$ in the similarity transformation should satisfy orthogonality conditions and have the same norm[22].

$$E_{\text{sim}} = \sum_{\mathbf{x}_i} \Big(\left(\mathbf{a}_1^{\mathrm{T}} \mathbf{a}_2\right)^2 + \left(\mathbf{a}_1^{\mathrm{T}} \mathbf{a}_3\right)^2 + \left(\mathbf{a}_2^{\mathrm{T}} \mathbf{a}_3\right)^2 + \left(\mathbf{a}_1^{\mathrm{T}} \mathbf{a}_1 - \mathbf{a}_2^{\mathrm{T}} \mathbf{a}_2\right)^2 + \left(\mathbf{a}_2^{\mathrm{T}} \mathbf{a}_2 - \mathbf{a}_3^{\mathrm{T}} \mathbf{a}_3\right)^2 + \left(\mathbf{a}_3^{\mathrm{T}} \mathbf{a}_3 - \mathbf{a}_1^{\mathrm{T}} \mathbf{a}_1\right)^2 \Big) \quad (3)$$

where $\mathbf{a}_1$, $\mathbf{a}_2$, and $\mathbf{a}_3$ denote the column vectors of $\mathbf{A}_i$. E_{sim} plays an important role not only in preferring pure rigid motions but also in adjusting local scales to ensure the reference model aligns with the target model well. This is essential in performing non-rigid registration between models of different sizes.

The additional regularization term E_{reg} ensures smoothness in deformation. Actually, E_{reg} sums two energies, specifically, $E_{reg} = E_{consist} + E_{smooth}$. The following regularization $E_{consist}$ allows us to yield consistent affine transformations and translations.

$$E_{\text{consist}} = \sum_{\mathbf{x}_i} \sum_{\mathbf{x}_j} \left\| \mathbf{A}_i (\mathbf{x}_j - \mathbf{x}_i) + \mathbf{x}_i + \mathbf{t}_i - (\mathbf{x}_j + \mathbf{t}_j) \right\|_2^2 \quad (4)$$

In addition, E_{smooth} is introduced to ensure that the transformation $\mathbf{T}_i$ associated with node $\mathbf{x}_i$ is compatible with those of adjacent nodes as follows:

$$E_{\text{smooth}} = \sum_{\mathbf{x}_i} \sum_{\mathbf{x}_j} \left\| \mathbf{A}_i (\mathbf{x}_j - \mathbf{x}_i) + \mathbf{A}_j (\mathbf{x}_i - \mathbf{x}_j) \right\|_2^2. \quad (5)$$

C. Pairwise Registration

To align the reference model toward the target model, we define another energy term E_{fit} that shifts graph nodes toward the corresponding positions. Given correspondences $\mathscr{C} = \{(\mathbf{x}_i, \mathbf{q}_i) | i \in 1 \cdots s\}$ where $\mathbf{q}_i$ denotes a vertex of the target model corresponding to graph node $\mathbf{x}_i$, E_{fit} penalizes distances between the corresponding pairs. Because the simple point-to-point metric may degrade the reference model, we project the displacements onto the normals of the nodes to suppress extreme deformations in the tangential directions[22]. Additionally, assuming the given correspondences $\mathscr{C}$ may contain bad corresponding pairs as is often the case with ICP, we associate a confidence variable ω_i with each node to evaluate the reliability. Specifically, E_{fit} is defined accompanied with an energy term E_{conf}[4] for regularization as follows:

$$E_{\text{fit}} = \sum_{i \in \mathscr{C}} {\omega_i}^2 \left\| \mathbf{x}_i - (\tilde{\mathbf{x}}_i + \mu_i \tilde{\mathbf{n}}_i) \right\|_2^2, \quad (6)$$

$$E_{\text{conf}} = \sum_{i \in \mathscr{C}} \left(1 - {\omega_i}^2\right)^2, \quad (7)$$

where $\tilde{\mathbf{x}}_i$ and $\tilde{\mathbf{n}}_i$ are the current position and normal of node $\tilde{\mathbf{x}}_i$ respectively, and μ_i is set as $\mu_i = (\mathbf{q}_i - \tilde{\mathbf{x}}_i) \cdot \tilde{\mathbf{n}}_i$. Note that each ω_i is treated as an unknown as well as the affine transformations to naturally eliminates bad correspondences that cause extreme deformations.

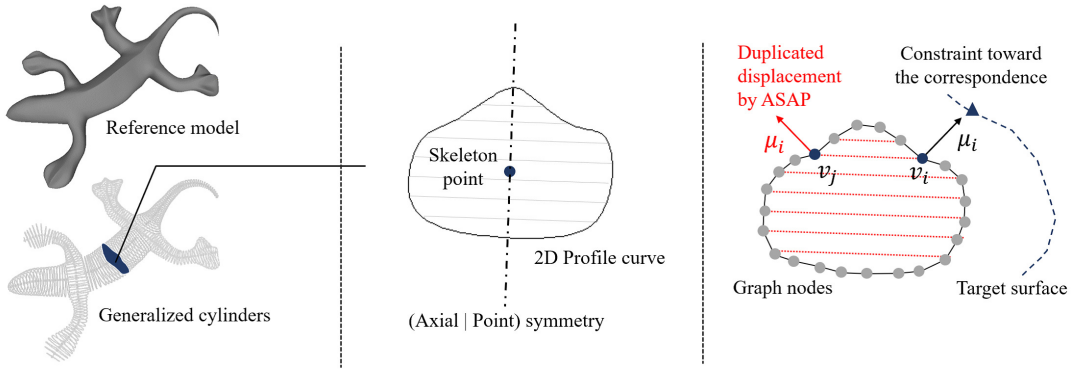

(a) Reference model decomposition (b) Local symmetry assumption (c) Symmetry-aware graph

Fig. 2. Symmetry constraint derived from generalized cylinders

D. Symmetry constraint via generalized cylinder decomposition

To better infer the missing surface, we pose an additional constraint concerning the symmetricity by leveraging the generalized cylinder. Cylindrical parts are ubiquitous in many natural and artificial objects. Therefore, the generalized cylinder, which is composed of pairs of skeletal and cross-section profile curves, covers a broad scope of object shapes[23][24][25]. We decompose the reference 3D model into generalized cylinders to analyze its symmetry, and build a symmetry-aware embedded graph so that displacements toward the partial observation affect the other side of the reference model to maintain the symmetric structure, thereby recover missing parts in more detail.

First, a reference mesh model is decomposed into a set of generalized cylinders following [8]. The generalized cylinder decomposition[8] progressively builds local to non-local cylinders and decides on a globally optimized combination of cylinders in a manner of the exact cover problem. It provides consistent skeletal and cross-section profile curves (see Fig. 1(c)), and enables us to analyze local symmetry.

As a next step, we introduce symmetry-aware edges in the embedded deformation graph based on the decomposition result. The embedded deformation graph is constructed through farthest-point sampling and K-nearest neighbors ($m = 400$ and $K = 4$ in all experiments) to approximate the reference model by a coarse mesh model. To preserve the symmetry of the reference model, we additionally connect symmetric nodes. Specifically, we use a skeleton point for a central symmetry, or extract an axial symmetry passing through the skeleton point that minimizes symmetry distance [26] on every 2D profile curve, and form symmetric point pairs in the generalized cylinders (Fig.2). The symmetric edges are then added in the deformation graph by approximating the point pairs with the closest nodes (Fig.1(d)).

Finally, for symmetry-aware deformation, we replace Equation (6) with the following ASAP energy term:

$$E_{\text{asap}} = \sum_{i \in \mathscr{C}} \omega_i{}^2 \left\{ \|\mathbf{x}_i - (\tilde{\mathbf{x}}_i + \mu_i \tilde{\mathbf{n}}_i)\|_2^2 + \left\|\mathbf{x}_j - (\tilde{\mathbf{x}}_j + \mu_i \tilde{\mathbf{n}}_j)\right\|_2^2 \right\}, \tag{8}$$

where $(\mathbf{x}_i, \mathbf{x}_j)$ are connected with a symmetric edge. ASAP allows the reference model to deform itself maintaining its underlying symmetry by duplicating displacements μ_i on another side; this leads to plausible shape completion in the area with no observation. Note that if the symmetric node $\mathbf{x}_j$ has its own position constraint, the latter symmetric constraint in Equation (8) is ignored to avoid inconsistent deformation.

E. Optimization

We define an objective function in the non-rigid registration by summing up the energy terms:

$$E = \alpha_{sim} E_{\text{sim}} + \alpha_{reg} E_{\text{reg}} + \alpha_{asap} E_{\text{asap}} + \alpha_{conf} E_{\text{conf}}. \tag{9}$$

The number of optimization variables is $13m$, corresponding to the affine transformations and confidences in the embedded deformation graph. We minimize Equation (9) by solving the nonlinear least-squares problem with the Gauss-Newton algorithm using Cholesky factorization. By alternating the energy minimization and correspondence determination, we gradually deform the reference model.

The optimization weights are initially set as $\alpha_{sim} = 100$, $\alpha_{reg} = 100$, $\alpha_{asap} = 10$, and $\alpha_{conf} = 10$, and α_{reg} is halved at every iteration until $\alpha_{reg} < 10$. We then remove the confidence variables ω and replace E_{asap} as the following energy term to pose the vertex-wise constraints; we then perform an iterative optimization again to capture the details of the target model according to vertex correspondences $\mathscr{C}^*$.

$$E^*_{\text{asap}} = \sum_{i \in \mathscr{C}^*} \left\{ \|\mathbf{v}_i - (\tilde{\mathbf{v}}_i + \mu_i \tilde{\mathbf{n}}_i)\|_2^2 + \left\|\mathbf{v}_j - (\tilde{\mathbf{v}}_j + \mu_i \tilde{\mathbf{n}}_j)\right\|_2^2 \right\}, \tag{10}$$

IV. Experiments

A. Results

We performed experiments to evaluate the performance of the proposed method. 3D models used in the experiments were obtained from a benchmark[27]. We first selected three models belonging to different categories as reference models to be deformed (Fig.3(a)). To evaluate the completion results

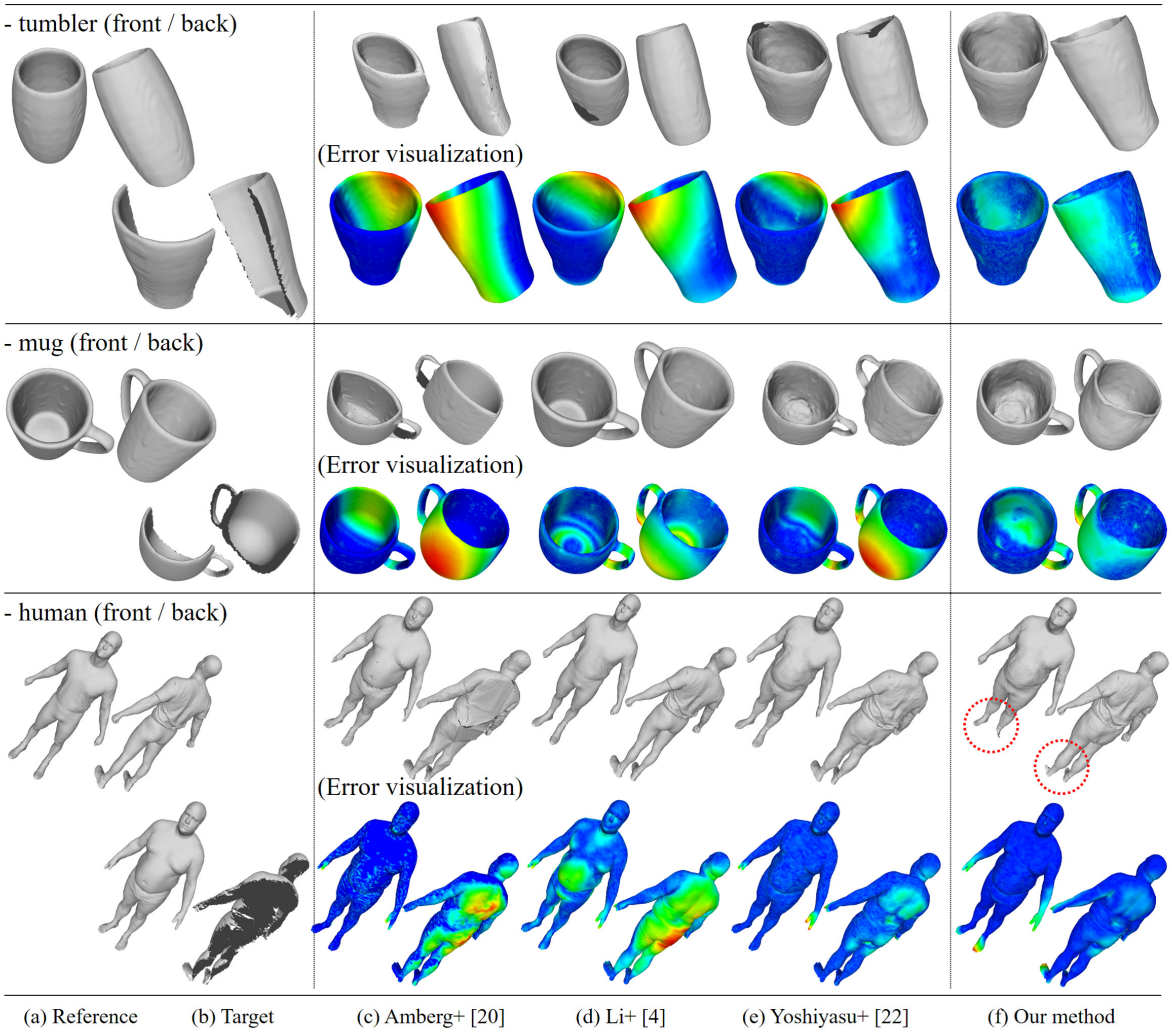

Fig. 3. Experimental results and error comparisons

quantitatively, we synthesized incomplete geometric data assuming partial observation (Fig.3(b)). Specifically, each incomplete model was used as a query and a reference model from the same category was deformed with non-rigid registration techniques to infer the entire shapes. The completion results were evaluated by calculating residual errors between the original and completed models based on vertex correspondences via nearest neighbor searches.

Note that the initial registration is performed manually so that the positions and rotations are roughly aligned, which can be replaced with conventional rigid registrations. Correspondences between the reference and target models are computed using closest point methods like ICP while eliminating invalid ones when the normal difference exceeds 40[deg], or the position difference exceeds 20% of the longest side of the bounding box of the reference model. In addition, we assume that the reference models in this experiment have local point-symmetric structures, and built point-symmetry-aware embedded graphs for ASAP.

Fig. 3(c)-(f) shows the completed 3D models with non-rigid registration techniques including the proposed method. Quantitative comparisons are also shown in Table I. Overall, the method of [20] aligned reference models well toward the query shapes, however, the other sides of the model significantly distorted. The non-rigid alignment technique [4] based on the embedded deformation did not work well because the method assumes isometric registration while the shapes of reference and target models in this experiments were substantially different. Although the approach of [22] provided better results by allowing similarity transformations for different size models, the other side of the deformed models still remained as in the original reference models. In contrast, our method restored the entire 3D models from the partial observation by making the graph nodes cooperate each other to retain the symmetry of the structure, which leads to better shape predictions.

B. Limitations

In the human case, the performance of the proposed method got worse compared with in the other cases. This may come from the poor description of the underlying symmetry as a result of the rough assumption of point-symmetry. Therefore, we perform an additional experiment

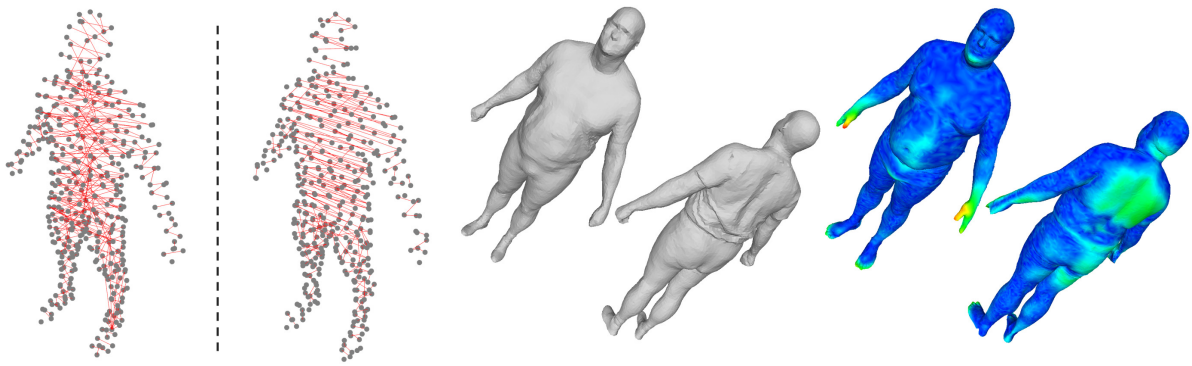

(a) Point-symmetry node graph (b) Axial-symmetry node graph (c) Non-rigid registration result with axial-symmetry-aware deformation (d) Residual errors

Fig. 4. Completion with an axial symmetry-aware graph

TABLE I

QUANTITATIVE COMPARISONS USING 3D MESH MODELS FROM [27]. THE ERRORS INDICATE AVERAGE AND MAX DISTANCES [%] FROM THE COMPLETE TARGET MODELS TO THE DEFORMED REFERENCE MODELS RELATIVE TO THE LONGEST SIDES OF THE BOUNDING BOXES.

Category	Reference	Target	RMS errors (average / max)			
			Amberg *et al.*[20]	Li *et al.*[4]	Yoshiyasu *et al.*[22]	Our method
tumbler	model 40	model 25	9.32 / 33.8	5.22 / 25.4	2.37 / 15.1	**1.32** / **9.08**
mug	model 27	model 33	6.03 / 26.9	3.12 / 14.8	3.65 / 18.1	**2.10** / **11.8**
human	model 2	model 13	0.557 / **4.22**	1.27 / 4.97	**0.508** / 5.23	0.708 / 9.36 (point-sym.) 0.625 / 4.87 (axial-sym.)

with an axial-symmetry-aware embedded graph. As shown in Fig. 4 and Table I, the graph represents the local symmetry in the reference model better, especially in the torso, and improved the completion performance. This implies that adaptive symmetry extraction is essential to obtain valid symmetry constraints.

In addition, as mentioned in [22], non-rigid shape matching should be used to register different size models. In the mug case, none of the registration techniques successfully aligned with the handle because of difficulty in obtaining valid correspondences via closest point method. Moreover, ASAP can largely shrink or inflate the partial shapes of the reference model when it couldn't get appropriate correspondences (See red circles in Fig. 3). Therefore, non-rigid matching like [28] should be used in the initial registration, and as well in the iterative optimization if needed, to boost the performance of the proposed method.

V. CONCLUSION

We proposed a method to infer an entire 3D shape from partial geometric data with a new non-rigid registration. By representing the reference model as a symmetry-aware deformation graph, we developed an effective non-rigid registration algorithm that tried to preserve the local symmetry and restore plausible surfaces.

For better performance in non-rigid registration of different size objects, we will improve the correspondence search and the symmetry extraction. In addition, while we currently focus only on local symmetry extracted via generalized cylinder decomposition, some objects also have global symmetry. Therefore, we will address shape inference using global and local symmetry simultaneously for better completion results.

REFERENCES

[1] J. Bohg, M. Johnson-Roberson, B. Len, J. Felip, X. Gratal, N. Bergstrm, D. Kragic, and A. Morales, "Mind the gap - robotic grasping under incomplete observation," in *IEEE International Conference on Robotics and Automation*, 2011, pp. 686–693.

[2] D. Rodriguez and S. Behnke, "Transferring Category-Based Functional Grasping Skills by Latent Space Non-Rigid Registration," *IEEE Robotics and Automation Letters*, vol. 3, no. 3, pp. 2662–2669, 2018.

[3] T. Matsubara and K. Shibata, "Active tactile exploration with uncertainty and travel cost for fast shape estimation of unknown objects," *Robotics and Autonomous Systems*, vol. 91, pp. 314 – 326, 2017.

[4] H. Li, R. W. Sumner, and M. Pauly, "Global Correspondence Optimization for Non-Rigid Registration of Depth Scans," *Computer Graphics Forum*, vol. 27, no. 5, pp. 1421–1430, 2008.

[5] H. Li, B. Adams, L. J. Guibas, and M. Pauly, "Robust Single-view Geometry and Motion Reconstruction," *ACM Trans. Graph.*, vol. 28, no. 5, pp. 175:1–175:10, Dec. 2009.

[6] M. Zollhöfer, M. Nießner, S. Izadi, C. Rehmann, C. Zach, M. Fisher, C. Wu, A. Fitzgibbon, C. Loop, C. Theobalt, and M. Stamminger, "Real-time Non-rigid Reconstruction Using an RGB-D Camera," *ACM Trans. Graph.*, vol. 33, no. 4, pp. 156:1–156:12, July 2014.

[7] K. Li, J. Yang, Y. Lai, and D. Guo, "Robust Non-Rigid Registration with Reweighted Position and Transformation Sparsity," *IEEE Transactions on Visualization and Computer Graphics*, pp. 1–1, 2018.

[8] Y. Zhou, K. Yin, H. Huang, H. Zhang, M. Gong, and D. Cohen-Or, "Generalized Cylinder Decomposition," *ACM Trans. Graph.*, vol. 34, no. 6, pp. 171:1–171:14, 2015.

[9] J. Rock, T. Gupta, J. Thorsen, J. Gwak, D. Shin, and D. Hoiem, "Completing 3D object shape from one depth image," in *IEEE Conference on Computer Vision and Pattern Recognition*, 2015, pp. 2484–2493.

[10] J.Varley, C.DeChant, A.Richardson, J.Ruales, and P.Allen, "Shape completion enabled robotic grasping," in *IEEE/RSJ International Conference on Intelligent Robots and System*, 2017, pp. 2442–2447.

[11] P.Schmidt, N.Vahrenkamp, M.Wchter, and T.Asfour, "Grasping of Unknown Objects using Deep Convolutional Neural Networks based on Depth Images," in *IEEE International Conference on Robotics and Automation*, 2018, pp. 6831–6838.

[12] Y. Ohtake, A. Belyaev, and H. Seidel, "A multi-scale approach to 3D scattered data interpolation with compactly supported basis functions," *Shape Modeling International*, pp. 153–161, 2003.

[13] D.Williams and A.Fitzgibbon, "Gaussian process implicit surfaces," 2007.

[14] S. Caccamo, Y. Bekiroglu, C. H. Ek, and D. Kragic, "Active exploration using Gaussian Random Fields and Gaussian Process Implicit Surfaces," in *IEEE/RSJ International Conference on Intelligent Robots and Systems*, 2016, pp. 582–589.

[15] D. Schiebener, A. Schmidt, N. Vahrenkamp, and T. Asfour, "Heuristic 3D object shape completion based on symmetry and scene context," in *2016 IEEE/RSJ International Conference on Intelligent Robots and Systems (IROS)*, 2016, pp. 74–81.

[16] P. Speciale, M. R. Oswald, A. Cohen, and M. Pollefeys, "A Symmetry Prior for Convex Variational 3D Reconstruction," in *European Conference on Computer Vision*, 2016.

[17] R.F.Salas-Moreno, R.A.Newcombe, H.Strasdat, P.H.J.Kelly, and A.J.Davison, "SLAM++: Simultaneous Localisation and Mapping at the Level of Objects," in *IEEE Conference on Computer Vision and Pattern Recognition*, 2013, pp. 1352–1359.

[18] C. Choi and H. I. Christensen, "RGB-D object tracking: A particle filter approach on GPU," in *2013 IEEE/RSJ International Conference on Intelligent Robots and Systems*, 2013, pp. 1084–1091.

[19] Z. Zeng, Y. Zhou, O. C. Jenkins, and K. Desingh, "Semantic Mapping with Simultaneous Object Detection and Localization," *2018 IEEE/RSJ International Conference on Intelligent Robots and Systems (IROS)*, pp. 911–918, 2018.

[20] B. Amberg, S. Romdhani, and T. Vetter, "Optimal Step Nonrigid ICP Algorithms for Surface Registration," in *IEEE Conference on Computer Vision and Pattern Recognition*, 2007, pp. 1–8.

[21] R. W. Sumner, J. Schmid, and M. Pauly, "Embedded Deformation for Shape Manipulation," *ACM Trans. Graph.*, vol. 26, no. 3, July 2007.

[22] Y. Yoshiyasu, W.-C. Ma, E. Yoshida, and F. Kanehiro, "As-Conformal-As-Possible Surface Registration," *Comput. Graph. Forum*, vol. 33, pp. 257–267, 2014.

[23] A. Tagliasacchi, H. Zhang, and D. Cohen-Or, "Curve Skeleton Extraction from Incomplete Point Cloud," *ACM Trans. Graph.*, vol. 28, no. 3, pp. 71:1–71:9, 2009.

[24] T. Chen, Z. Zhu, A. Shamir, S.-M. Hu, and D. Cohen-Or, "3 Sweep: Extracting Editable Objects from a Single Photo," *ACM Trans. Graph.*, vol. 32, no. 6, pp. 195:1–195:10, 2013.

[25] K. Yin, H. Huang, H. Zhang, M. Gong, D. Cohen-Or, and B. Chen, "Morfit: Interactive Surface Reconstruction from Incomplete Point Clouds with Curve-driven Topology and Geometry Control," *ACM Trans. Graph.*, vol. 33, no. 6, pp. 202:1–202:12, 2014.

[26] J. Podolak, P. Shilane, A. Golovinskiy, S. Rusinkiewicz, and T. Funkhouser, "A Planar-reflective Symmetry Transform for 3D Shapes," *ACM Trans. Graph.*, vol. 25, no. 3, pp. 549–559, July 2006.

[27] X. Chen, A. Golovinskiy, and T. Funkhouser, "A Benchmark for 3D Mesh Segmentation," *ACM Transactions on Graphics*, vol. 28, no. 3, 2009.

[28] Y. Yoshiyasu, E. Yoshida, K. Yokoi, and R. Sagawa, "Symmetry-Aware Nonrigid Matching of Incomplete 3D Surfaces," in *2014 IEEE Conference on Computer Vision and Pattern Recognition*, 2014, pp. 4193–4200.